

Low lying excited states of ^{24}O investigated by self-consistent microscopic description of proton inelastic scattering

Kazuhito Mizuyama* and Kazuyuki Ogata

Research Center for Nuclear Physics, Osaka University, Ibaraki 567-0047, Japan

(Dated: July 9, 2018)

The proton inelastic scattering of $^{24}\text{O}(p, p')$ at 62 MeV/nucleon is described by a self-consistent microscopic calculation with the continuum particle-vibration coupling (cPVC) method. The SLy5, SkM*, and SGII parameters are adopted as an effective nucleon-nucleon interaction. For all the parameters, the cPVC calculation reproduces very well the first peak at 4.65 MeV in the ^{24}O excitation energy spectrum as well as its angular distribution. The role of the cPVC self-energy strongly depends on the effective interactions. The higher-lying strength around 7.3 MeV is suggested to be a superposition of the 3^- and 4^+ states by the results with SLy5 and SGII, whereas the SkM* calculation indicates it is a pure 3^- state. This difference gives a rather strong interaction dependence of the angular distribution corresponding to the higher-lying strength.

PACS numbers: 21.60.Jz, 24.10.Eq, 24.10.Ht, 25.60.Bx, 25.60.Dz

Elucidation of particle-unbound excited states of neutron-dripline nuclei is a hot subject in nuclear physics. It provides us with rich information on the dripline nuclei that is difficult to extract from their ground state properties. Very recently, proton inelastic cross sections of ^{24}O at 62 MeV/nucleon were measured [1]. The spin parity λ^π of the first excited state at 4.65 ± 0.14 MeV was assigned 2^+ and the quadrupole transition parameter β_2 turned out to be small ($\beta_2 = 0.15 \pm 0.04$). The large shell gap at $N = 16$ (N is the neutron number) was thus confirmed. Another interesting finding of the measurement was the strong (relatively-) higher-lying strength around 7.3 MeV considered to have negative-parity configurations. This strength was suggestive of the quenching of the gap between the sd and fp shells of neutron. For more detailed discussion, clarification of the λ^π of the higher-lying strength will be necessary. Fully microscopic description of the proton inelastic cross sections of ^{24}O is crucial for this purpose.

In a recent paper [2], the continuum particle-vibration coupling (cPVC) method was proposed and applied to studies on the single-particle (sp) structures in ^{40}Ca , ^{208}Pb , and ^{24}O . It was shown in Ref. [2] that the cPVC method describes quite well the fragmentation of the sp hole and particle states as well as the shift of those centroid energies, in good agreement with the experimental spectroscopic factor.

We then applied the cPVC method to the neutron elastic scattering on ^{16}O at 4–30 MeV and succeeded in reproducing experimental data of the total-elastic cross section σ_{el} and the reaction cross section σ_{R} satisfactorily well [3]. The cPVC method treats the neutron single-particle motion and the vibration of the ^{16}O nucleus in a unified manner. One of the remarkable aspects of the cPVC method for the $n + ^{16}\text{O}$ system is that the important properties of the neutron optical potential, i.e., energy dependence, complex nature, and non-locality, are automatically generated within a coupled-channel framework using an energy-independent and real nucleon-nucleon effective interaction. This gives a fully microscopic self-consistent description of nucleon-nucleus scattering. Furthermore, the

cPVC method can describe even doorway states [4] of the nucleon-nucleus system that are observed as narrow peaks in the total reaction cross section. It is well known that such states cannot be described by a phenomenological optical potentials or by a folding model calculation based on a complex g matrix [5–13].

In the description of neutron elastic scattering by the cPVC method, large numbers of discrete and continuum phonon states of the core nucleus (or target in a terminology of reaction studies) are explicitly taken into account. Therefore, it is quite straightforward to extend the cPVC method to inelastic scattering processes. The purpose of the present work is to apply the cPVC method to the proton inelastic scattering by ^{24}O and to discuss the spin-parity of the higher-lying strength around 7.3 MeV observed.

The double differential cross section for the proton-nucleus inelastic scattering is given by

$$\frac{d^2\sigma}{dE_x d\Omega} = - \left(\frac{4m}{\hbar^2} \right)^2 \frac{k_f}{k_i} \sum_{\lambda} \text{Im} \sum_{l_f l_i} \sum_{l'_f l'_i} \mathcal{P}_{\lambda}^{l_f l_i; l'_f l'_i}(\cos \theta) \times \int dr \int dr' \langle C \kappa_{l_f l_i}^{\lambda}(r) \rangle^* R_{\lambda}(r, r'; E_x) \langle C \kappa_{l'_f l'_i}^{\lambda}(r') \rangle, \quad (1)$$

where

$$\langle C \kappa_{l_f l_i}^{\lambda}(r) \rangle \equiv \sum_{j_f j_i} C_{l_f j_f; l_i j_i}^{\lambda} \langle \phi_{l_f j_f}^{\text{HF}}(k_f) | | \kappa(r) | | \psi_{l_i j_i}(k_i) \rangle, \quad (2)$$

$$C_{l_f j_f; l_i j_i}^{\lambda} \equiv \frac{(-)^{j_i + l_f + \frac{1}{2} + \lambda} \widehat{j_f} \widehat{j_i}}{\sqrt{2} \widehat{\lambda}^3} \times \langle l_f j_f | | Y_{\lambda} | | l_i j_i \rangle \left\{ \begin{array}{ccc} l_i & j_i & 1/2 \\ j_f & l_f & \lambda \end{array} \right\}, \quad (3)$$

$$\langle \phi_{l_f j_f}^{\text{HF}}(k_f) | | \kappa(r) | | \psi_{l_i j_i}(k_i) \rangle \equiv i^{l_i} (i^{l_f})^* \phi_{HF, l_f j_f}^*(r; k_f) \frac{\kappa(r)}{r^2} \psi_{l_i j_i}(r; k_i), \quad (4)$$

*Electronic address: mizukazu147@gmail.com

and

$$\begin{aligned} & \mathcal{P}_\lambda^{l_f l_i; l'_f l'_i}(\cos \theta) \\ & \equiv \sum_I \hat{\lambda}^2 \left\{ \begin{matrix} l_i & l_f & \lambda \\ l'_f & l'_i & I \end{matrix} \right\} \langle l'_i || Y_I || l_i \rangle \langle l'_f || Y_I || l_f \rangle P_I(\cos \theta). \end{aligned} \quad (5)$$

The excitation energy of the target nucleus is denoted by $E_x = E_i - E_f$ with $E_c = \hbar^2 k_c^2 / (2m)$; m is the nucleon mass and k_c is the wave number of proton. $c = i$ and f represent the initial and final states, respectively. The orbital (total) angular momentum of proton is denoted by l_c (j_c). $\psi_{l_i j_i}$ is the cPVC scattering wave function obtained by solving the cPVC Lippmann-Schwinger equation [3]. We use $\psi_{l_i j_i}$ in the transition matrix as the total wave function of the system in the initial state. $\phi_{l_f j_f}^{\text{HF}}(k_f)$ is the Hartree-Fock (HF) scattering wave function, R_λ is the response function calculated by the continuum random phase approximation (RPA) [14, 15], and $\kappa(r)$ is the residual interaction. For simplicity, we disregard the spin-dependent terms of the residual interaction in the calculation of RPA and cPVC self-energy. The momentum-dependent terms are taken into account self-consistently in RPA, but the Landau-Migdal (LM) approximation [2] is adopted in the calculation of the self-energy. Furthermore, the residual Coulomb interaction is dropped in the self-energy function. The Feynman diagram corresponding to Eq. (1) is shown in Fig. 1.

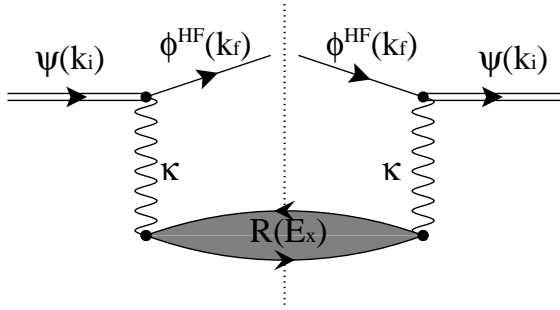


FIG. 1: The Feynman diagram corresponding to the double differential cross section for the nucleon-nucleus inelastic scattering expressed by Eq. (1). ϕ^{HF} and ψ are the HF and cPVC scattering wave functions, respectively. κ is the residual force. $R(E_x)$ is the continuum RPA response function. The half part of the diagram expresses the transition matrix.

In the present study, the RPA phonons of $\lambda^\pi = 1^-, 2^+, 3^-, 4^+$, and 5^- are included and the maximum excitation energy of ^{24}O is taken to be 60 MeV. The angular momentum cut-off l_{max} for the single-particle orbits is set to 12. As the nucleon-nucleon effective interaction, we take SLy5 [16], SkM* [17], and SGII [18] Skyrme parameters, and discuss the interaction dependence of the inelastic cross section. We choose the Fermi momentum $k_F = 1.33 \text{ fm}^{-1}$ for the residual force with the LM approximation. The radial mesh size is 0.2 fm and the maximum value of r in the inelastic in Eq. (1) is set to 20 fm.

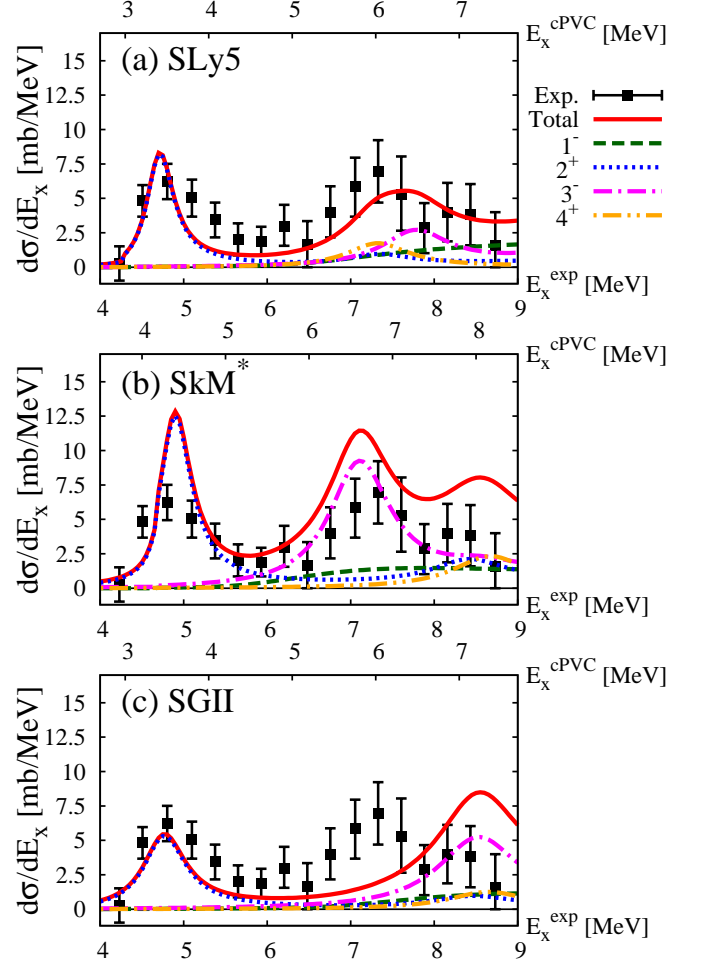


FIG. 2: (Color online) The differential cross section $d\sigma/dE_x$ plotted as a function of the excitation energy E_x of ^{24}O for the (p, p') reaction at 62 MeV/nucleon, and compared with the experimental data [1]. Panels (a), (b), and (c) are the results with the SLy5, SkM*, and SGII Skyrme interaction, respectively. The solid line is the total energy spectrum. The dashed, dotted, dash-dotted and dash-dot-dotted lines are the contributions from the 1^- , 2^+ , 3^- , and 4^+ states of ^{24}O , respectively, in each panel. The lower horizontal axis is the experimental excitation energies of ^{24}O , E_x^{exp} , and the upper axis is the theoretical one, E_x^{cPVC} . See the text for detail.

In Fig. 2 we show the energy spectra of the $^{24}\text{O}(p, p')$ reaction at 62 MeV calculated by the cPVC method with the (a) SLy5, (b) SkM*, and (c) SGII interactions. In each panel, the solid line is the total energy spectrum plotted as a function of E_x and compared with the experimental data; the dashed, dotted, dash-dotted, and dash-dot-dotted lines respectively show the contributions from the 1^- , 2^+ , 3^- , and 4^+ states of ^{24}O . We have smeared the theoretical results taking account of the experimental resolution $0.5\sqrt{E_x - 4.09}$ in FWHM given in Ref. [1]. Additionally, we have shifted the theoretical cross sections obtained with the SLy5 and SGII interactions by $\Delta E_x = 1.3 \text{ MeV}$ toward the high E_x direction, to adjust its

first peak to that of the experimental data; for the result with SkM*, $\Delta E_x = 0.5$ MeV is used. We have not renormalized the absolute values of the cross sections shown in this paper. One sees from Fig. 2 that for SLy5 and SkM* the cross sections calculated agree well with the experimental data, which shows the success of the cPVC method in describing the proton inelastic scattering. When SGII is used, however, the relative energy between the two peaks is not reproduced well. For all the interactions, the first peak around 4.65 MeV is found to be purely the 2^+ state of ^{24}O , as confirmed in Ref. [1].

There seems to be a missing strength for $5 \text{ MeV} \lesssim E_x \lesssim 6 \text{ MeV}$ for the results with the SLy5 and SGII interactions. This strength may be due to contributions from unnatural parity states, the 1^+ state in particular, which are not included in the present calculation. It was claimed in Ref. [1] that the 1^+ contribution was too small to explain the strength around $5 \text{ MeV} \lesssim E_x \lesssim 6 \text{ MeV}$, which is suggested by also an RPA calculation [19], and it might be due to the contribution of negative parity states. The dashed and dash-dotted lines in Figs. 2(a) and 2(c) indicate that there is no contribution of the negative parity states in this region. On the other hand, we have no such missing strength when the SkM* interaction is used. In panel (b) the peak around 4.65 MeV is due to almost the 2^+ state, with a small background of the 3^- state. Thus, the result for $5 \text{ MeV} \lesssim E_x \lesssim 6 \text{ MeV}$ shows the effective interaction dependence.

The interaction dependence is more significant for the higher-lying strength around 7.3 MeV. If SLy5 is used it is a superposition of the 3^- and 4^+ strengths added by the 1^- and 2^+ background contributions. On the other hand, the strength almost comes from the 3^- state when SkM* is adopted. The result with the SGII interaction is qualitatively the same as that with SkM*. However, the relative energy between the two peaks is not properly obtained as mentioned above. It should be noted that Skyrme parameters are determined to reproduce the properties of the ground state and giant resonances of nuclei in middle- and heavy-mass regions. On the other hand, it is rather well known that the low-lying excited states are more sensitive to the shell structure and may not necessarily be described well by the Skyrme interactions. Therefore, it is not surprising that the reaction observables associated with the low-lying states of the target nucleus show rather strong dependence on the Skyrme parameters. Considering this, the success of the cPVC method with Skyrme interactions in reproducing the experimental data will be quite remarkable, though there remain some discrepancies between the calculations and the experimental data. It will be interesting and important to use reaction observables as new constraints on the Skyrme parameters.

Figure 3(a) shows the angular distribution corresponding to the first 2^+ peak at $E_x = 4.65 \pm 0.14$ MeV. The results with SLy5, SkM*, and SGII are plotted by the solid, dashed, and dotted lines, respectively. One sees all the calculations perfectly reproduce the experimental data; the interaction dependence seems very small. However, if we see the coupled-channel effects, a clear interaction dependence appears. The results shown in Fig. 3(b) correspond to a one-step transition from the HF ground state of ^{24}O to its RPA 2^+ state; the mo-

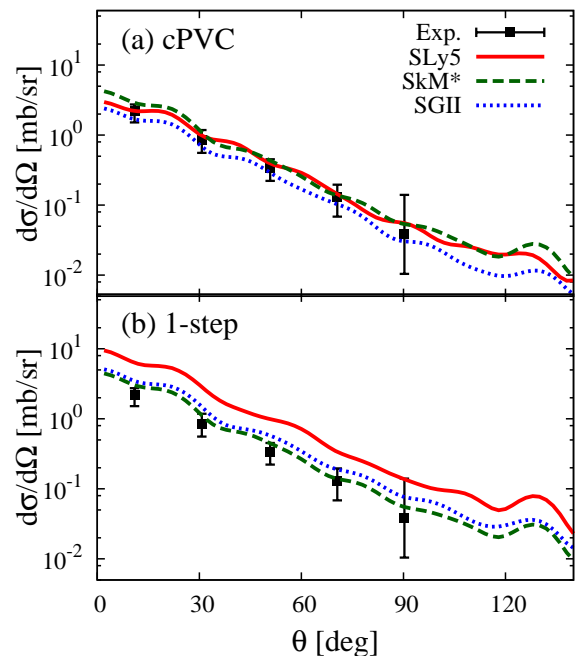


FIG. 3: (Color online) The angular distribution of the cross section $d\sigma/d\Omega$ corresponding to the first 2^+ state of ^{24}O at $E_x = 4.65 \pm 0.14$ MeV compared with the experimental data [1]. The solid, dashed, and dotted lines are the results with the SLy5, SkM*, and SGII respectively. Panels (a) and (b) are the results by the cPVC and a one-step transition respectively (see text).

tion of the incoming (outgoing) proton is described by a mean-field potential generated by the ground (RPA 2^+) state of ^{24}O . In other words, only the folding part of an optical potential is included dropping all the dynamical polarization potentials (DPPs). Note that this one-step calculation is different from a usual DWBA calculation that adopts the proton-target distorting (optical) potentials including DPPs in the initial and final channels. The solid line in Fig. 3(b) is significantly larger than that in Fig. 3(a), mainly because of the absence of absorption, i.e., the imaginary part of the optical potential. A similar difference is found in the results with the SGII interaction. On the other hand, the one-step calculation with SkM* is almost the same as the result of the cPVC calculation. This indicates that there is no absorption of the flux of the incident proton when SkM* is adopted, which is quite difficult to understand. If this is indeed the case, the proton elastic scattering on ^{24}O can be described by only the HF single-particle potential, suggesting a very small value of reaction cross section.

The effective-interaction dependence of the result will be investigated more clearly if the angular distribution of the higher-lying states is obtained. Figure 4 shows the theoretical results of the angular distribution; panels (a) and (b) correspond to the energy regions of $7 \text{ MeV} \leq E_x \leq 7.5 \text{ MeV}$ and $7.5 \text{ MeV} \leq E_x \leq 8 \text{ MeV}$, respectively. The solid (dashed) line in each panel shows the result calculated with the SLy5 (SkM*) interaction. The shape of the solid line in panel (a) is quite different from that in panel (b). This is because, as

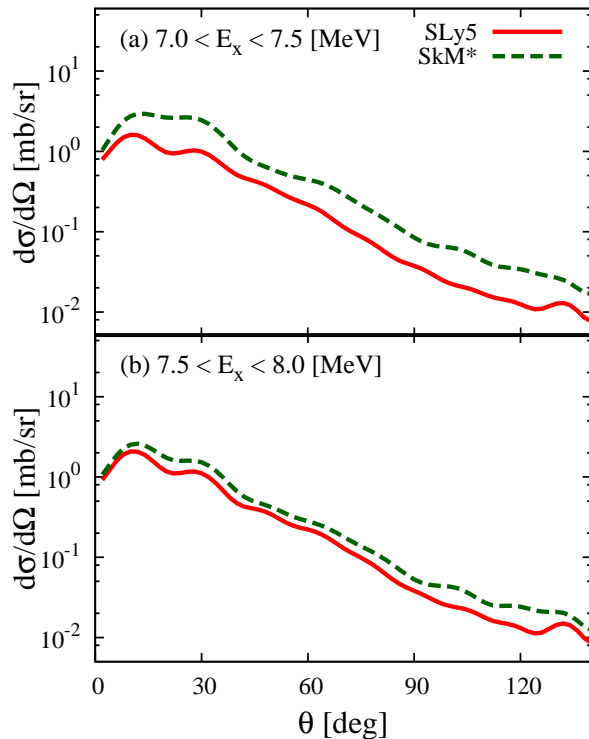


FIG. 4: (Color online) The angular distributions correspond to (a) $7 \text{ MeV} \leq E_x \leq 7.5 \text{ MeV}$ and (b) $7.5 \text{ MeV} \leq E_x \leq 8 \text{ MeV}$. In each panel the solid and dashed lines show the results with the SLy5 and SkM* interactions, respectively.

shown in Fig. 2(a), the spin-parity of ^{24}O having the largest contribution is 4^+ for $7 \text{ MeV} \leq E_x \leq 7.5 \text{ MeV}$ and 3^- for $7.5 \text{ MeV} \leq E_x \leq 8 \text{ MeV}$ when SLy5 is adopted. On the other hand, the results with SkM* (the dashed lines) have a similar shape, reflecting the fact that the 3^- state has a dominant contribution in both energy ranges, as shown in Fig. 2(b). In Fig. 5 we decompose the results in Fig. 4(a) into the contributions of the 3^- and 4^+ states. Clearly, the difference in the 4^+ state contributions for SLy5 and SkM* gives the different angular distributions for $7 \text{ MeV} \leq E_x \leq 7.5 \text{ MeV}$. Comparison with experimental data will be very interesting and important.

In summary, we have applied the cPVC method to the $^{24}\text{O}(p, p')$ reaction at 62 MeV/nucleon. We took the SLy5, SkM*, and SGII parameters as an effective nucleon-nucleon interaction. For all the three parameters, the cPVC calculation well reproduces the experimental data of the energy spectrum and the angular distribution corresponding to the first 2^+ state, except that the relative energy between the two peaks cannot be reproduced when SGII is adopted. One finds that the calculations underestimate the strength at $5 \text{ MeV} \lesssim E_x \lesssim 6 \text{ MeV}$

when SLy5 or SGII is adopted, which may imply some contributions from unnatural parity states. On the other hand, there is no missing strength in that region when SkM* is used. The role of the cPVC self-energy, i.e., the dynamical polarization potential, has a strong dependence on the effective interac-

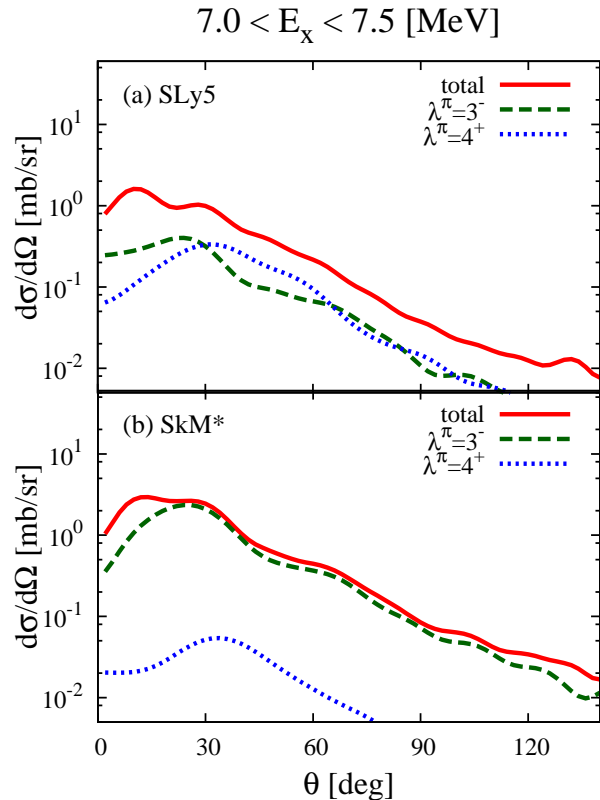


FIG. 5: (Color online) The contribution of the 3^- (dashed line) and 4^+ (dotted line) states to the angular distribution for $7.0 \leq E_x \leq 7.5 \text{ MeV}$ shown by Fig. 4(a). Panels (a) and (b) correspond to the results with SLy5 and SkM*, respectively.

tions. The higher-lying strength around 7.3 MeV is found to be a superposition of the 3^- and 4^+ states by the calculation with SLy5 and SGII, whereas the SkM* calculation indicates the strength is almost due to the 3^- state. Reflecting this difference, the shape of the angular distribution of the higher-lying strength has a rather strong dependence on the effective interaction. Experimental data for this distribution may judge which interaction is preferable for describing the proton inelastic scattering.

The authors thank G. Colò, E. Vigezzi, T. Inakura, H. Nakada, and M. Yahiro for helpful discussions. This research was supported in part by Grant-in-Aid of the Japan Society for the Promotion of Science (JSPS).

[1] K. Tshoo, *et al.*, Phys. Rev. Lett **109**, 022501(2012).

[2] K. Mizuyama, G. Colò, and E. Vigezzi, Phys. Rev. C **86**,

034318 (2012).

[3] K. Mizuyama and K. Ogata, Phys. Rev. C **86**, 041603(R)(2012).

- [4] C. F. Weisskopf, Phys. Today **14**, 18 (1961).
- [5] P. K. Deb, B. C. Clark, S. Hama, K. Amos, S. Karataglidis, and E. D. Cooper, Phys. Rev. C **72**, 014608 (2005).
- [6] L. Ray, G. W. Hoffmann, and W. R. Coker, Phys. Rep. **212**, 223 (1992).
- [7] E. D. Cooper, S. Hama, B. C. Clark, and R. L. Mercer, Phys. Rev. C **47**, 297 (1993).
- [8] L. Rikus, K. Nakano and H. V. von Geramb, Nucl. Phys. **A414**, 413 (1984).
- [9] L. Rikus and H.V. von Geramb, Nucl. Phys. **A426**, 496 (1984).
- [10] K. Amos, P. J. Dortmans, H. V. von Geramb, S. Karataglidis, and J. Raynal, Adv. Nucl. Phys. **25**, 275 (2000).
- [11] P. K. Deb and K. Amos, Phys. Rev. C **62**, 024605 (2000).
- [12] S. P. Weppner, Ch. Elster, and D. Huber, Phys. Rev. C **57**, 1378 (1998) and references therein.
- [13] T. Furumoto, Y. Sakuragi, and Y. Yamamoto, Phys. Rev. C **78**, 044610 (2008), *ibid.*, C **79**, 011601(R) (2009), *ibid.*, C **80**, 044614 (2009).
- [14] K. Mizuyama, M. Matsuo, and Y. Serizawa, Phys. Rev. C **79**, 024313 (2009).
- [15] H. Sagawa, Prog. Theor. Phys. Suppl. **142**, 1 (2001).
- [16] E. Chabanat, P. Bonche, P. Haensel, J. Meyer and R. Schaeffer, Nucl. Phys. **A635**, 231 (1998).
- [17] J. Bartel, P. Quentin, M. Brack, C. Guet and H. -B. Håkansson, Nucl. Phys. **A386**, 79 (1982).
- [18] Nguyen Van Giai and H. Sagawa, Nucl. Phys. **A371**, 1(1981).
- [19] T. Inakura, private communication (2013).